Radiation Effects and Their Annealing in Co^{60}-Gamma-Irradiated Sb-Doped Germanium

J. C. Pigg* and J. H. Crawford, Jr.
Solid State Division, Oak Ridge National Laboratory,† Oak Ridge, Tennessee
(Received 18 March 1964)

The annealing of changes in the electrical properties of antimony-doped germanium caused by Co^{60} gamma irradiation at 77°K has been investigated by both isochronal and isothermal techniques. The previously observed levels at 0.2 eV below the conduction band and near or below the middle of the forbidden band were studied individually. It was found that both the rate of carrier removal and the subsequent course of recovery upon annealing above 273°K were markedly dependent upon the antimony concentration (N_{Sb}). The rate of electron removal ($dn/d\phi t$) is smaller for lower antimony concentrations. Upon annealing in the range between 273 and 450°K, two distinct stages are observed. Stage A accounts for the major recovery of the change in carrier concentration for samples with high antimony concentration ($N_{Sb}=10^{15}$ cm^{-3}) and for the major recovery of reciprocal mobility for both high- and low-purity material. By contrast, the major recovery of carrier concentration for the low antimony concentrations ($N_{Sb}\approx10^{14}$ cm^{-3}) occurs in the high-temperature stage, stage B. Stage B proceeds with an apparent activation energy of $\sim$ 1.2 eV. The annealing data are considered in terms of a model in which the formation of antimony-vacancy and antimony-divacancy complexes occur as parallel processes to vacancy capture by sinks. A new energy level at 0.09 eV below the conduction band was observed after annealing at 370°K. The level has been tentatively attributed to oxygen-vacancy complexes.

INTRODUCTION

RECENT studies have shown that defect-impurity interactions play a dominant role in determining the nature of radiation effects and their subsequent thermal recovery in electron-bombarded silicon. From electron paramagnetic resonance (EPR) experiments, a dominant-acceptor state in oxygen-contaminated silicon (crucible-grown crystals) has been identified with a vacancy-oxygen complex.[1] The center is paramagnetic when its state 0.17 eV below the conduction band is occupied by an electron. The identification has been further substantiated by polarized infrared absorption measurements on crystals made birefringent by the application of uniaxial stress.[2] Moreover, Watkins and Corbett[3] have shown that the vacancy-donor complex is responsible for another important acceptor state $\sim$0.4 eV below the conduction band which controls the electronic behavior in irradiated *n*-type silicon with low oxygen content (floating-zone crystals). Although the oxygen-vacancy complex exhibits a high thermal stability, Saito *et al.*[4] have found that the donor-vacancy complex anneals in the range 393 to 423°K with an activation energy of 0.94 eV. Perhaps the most striking aspect of these studies is the fact that there is no evidence of any energy-state stable in the room-temperature range which can be attributed to an isolated vacancy or an isolated interstitial. In fact, Watkins[5] has shown that the mobility of vacancies (which act as donors in *p*-type silicon) is so high that they migrate to annihilation sites or interact with impurity atoms at temperatures in the range 120 to 160°K.

In view of its basic similarity to silicon in both crystal structure and electronic behavior, analogous processes might be expected to occur in irradiated germanium. Unfortunately, the latter is not nearly so amenable to study by EPR methods. However, from investigation of the thermal annealing of radiation-induced changes in carrier concentration, mobility, and minority carrier lifetime, the conclusion that defect-impurity complexes play an important role is inescapable. Brown and co-workers[6] made a careful study of the annealing of damage in electron (1.1 MeV) bombarded *n*-type germanium at 77°K. They found that the extent of recovery of carrier concentration in the first annealing stage (stage A) observed upon warming from the irradiation temperature was markedly influenced by the chemical identity of the donor atom. Stage A, which occurs in the range from 300 to 360°K with an activation energy between 0.75 and 0.8 eV, was found to account for $\sim$70% recovery in antimony-doped specimens, but for only 20 to 30% recovery in arsenic-doped specimens. The residual change in carrier concentration recovered only after annealing to higher temperatures. Moreover, in the same annealing range, the recovery of mobility was found to be quite different for the two types of donors: In the antimony-doped specimens, the mobility and the carrier concentration recovered together, whereas in the arsenic-doped speci-

* This work was done in partial fulfillment of the requirements for the degree Doctor of Philosophy at the University of Tennessee. Previously reported in ORNL-3443, May 1963 (unpublished).

† Oak Ridge National Laboratory is operated by Union Carbide Corporation for the U. S. Atomic Energy Commission.

[1] G. D. Watkins and J. W. Corbett, Phys. Rev. **121**, 1001 (1961).

[2] J. W. Corbett, G. D. Watkins, R. M. Chrenko, and R. S. McDonald, Phys. Rev. **121**, 1015 (1961).

[3] G. D. Watkins and J. W. Corbett, Discussions Faraday Soc. **31**, 86 (1961).

[4] H. Saito, M. Hirata, and J. Horiuchi, J. Phys. Soc. Japan **18**, 246 (1963); H. Saito and M. Hirata, Japanese J. Appl. Phys. **2**, 678 (1963).

[5] G. D. Watkins, J. Phys. Soc. Japan **18**, Suppl. 2, 22 (1962).

[6] W. L. Brown, W. M. Augustyniak, and T. R. Waite, J. Appl. Phys. **30**, 1258 (1956).

mens the mobility recovered completely, while only ~25% of the change in carrier concentration annealed. These results strongly suggest that the annealing properties are controlled by an interaction between the radiation produced defects and the impurity atoms present in the crystal.

Evidence for a defect-impurity interaction was also obtained by Curtis and Crawford[7] who found that the extent of recovery and the shape of the isochronal recovery curve for the minority carrier lifetime was strongly dependent upon the impurity concentration as well as whether the donor impurity is antimony or arsenic. The lifetime results showed that recovery analogous to the stage A annealing observed by Brown and co-workers dominated the annealing of antimony-doped specimens only if the donor concentration exceeded $\sim 3\times10^{14}$ cm^{-3}. For high-purity arsenic- and antimony-doped specimens ($<2\times10^{14}$ donors/cm^3), stage A accounted for only a minor portion of the recovery during isochronal annealing; most of the recovery occurred in the range above 400°K (stage B). The activation energy of stage A was found to be ~0.8 to 0.9 eV in reasonable agreement with the value obtained by Brown *et al.*

A series of isochronal and isothermal anneals on high-purity ($\sim 4\times10^{13}$ cm^{-3}) arsenic- and antimony-doped germanium have been reported by Ishino *et al.*[8] The samples were irradiated at 20°C with Co^{60} gamma rays. (Some of the samples were allowed to stand several days before annealing; consequently, the low activation-energy processes had time to decay before the start of the annealing cycles began.) These studies confirm that the nature of the impurity influences the course of recovery, but the effect is qualitatively quite different from that observed by Brown *et al.*[6] They found a multistage recovery (stages A and B discussed above refer to III_n and IV_n, respectively, in the notation of Ishino *et al.*). They find an activation energy of 0.7 −0.8 eV for stage III_n and ~1.2 eV for stage IV_n. The dominant recovery occurred in stage B (IV_n) rather than in stage A (III_n) in accord with the lifetime annealing results obtained on specimens with similar donor concentrations by Curtis and Crawford.[7]

This paper describes a detailed study of the annealing behavior of antimony-doped germanium. The main aim of the investigation was to elucidate the mechanisms underlying the various annealing stages and to explore the nature of impurity-defect interactions during thermal recovery of irradiated *n*-type germanium.

EXPERIMENTAL PROCEDURE

The samples explored in these studies were *n*-type germanium with antimony concentrations of 1.4×10^{14} and 1×10^{15} cm^{-3}. Disks were cut from the ingot perpendicular to the direction of growth. Bridge-type samples were cut from the central portions of the disks using an ultrasonic cutting die. The samples were then polished and etched with CP-4 etch. The dislocation density, determined from the etch pit counts, was $\sim10^4$ cm^{-2}. After applying Ohmic contacts with solder, the samples were checked for concentration gradients and only those of high uniformity were used.

Hall coefficient R and resistivity ρ measurements were made as a function of temperature over the range 77 to 300°K prior to irradiation. Irradiations were conducted in a Co^{60} gamma-ray source whose intensity at the sample, as measured by cerous sulfate dosimetry, was 1.94×10^{12} photons cm^{-2} sec^{-1}. During irradiation the samples were kept immersed in liquid nitrogen. In certain experiments specimens were withdrawn periodically for measurements of R and ρ. In most cases the accumulated exposures were sufficient to reduce the carrier concentration to ~10% of the original value.

Both isochronal (20-min pulses) and isothermal anneals were carried out for a series of specimens with 1.4×10^{14} antimony atoms cm^{-3}. Only isochronal anneals were performed on the 1×10^{15} cm^{-3} series since these indicated that the annealing behavior was almost identical to that reported by Brown *et al.*[6] After each heating pulse, the specimens undergoing isochronal anneal were cooled to a reference temperature for measurement of the property changes.

Cleland *et al.*[9,10] observed two levels in *n*-type germanium exposed to Co^{60} γ rays at room temperature, which are produced in essentially equal concentrations and are located 0.23 eV below the conduction band and near or below the middle of the band gap. Subsequent work has shown that the 0.2-eV level can be removed in some samples by annealing at 373°K without a corresponding decrease of the total concentration of defect-acceptor states. In fact, some samples showed an increase in deep-state concentration during the removal of the 0.2-eV states. In view of these results, it was felt that an independent examination of the recovery behavior of each class of states (both the deep and shallow) is essential. Therefore, wherever possible care was taken to determine the behavior of each group of states separately. This was accomplished as follows:

Until the temperature reached 273°K, only one reference point of 77°K was used, but after warming above 273°K, both this and 77°K were used as reference points. This procedure permitted the separate examination of the annealing of shallow-acceptor states (occupied only at the lower reference) and deep-acceptor states (occupied at both 77 and 273°K). The isothermal anneals were conducted in the range from 377 to 455°K.

[7] O. L. Curtis, Jr., and J. H. Crawford, Jr., Phys. Rev. **126**, 1342 (1962).
[8] S. Ishino, F. Nakazawa, and R. R. Hasiguti, Phys. Chem. Solids **24**, 1033 (1963).
[9] J. W. Cleland, J. H. Crawford, Jr., and D. K. Holmes, Phys. Rev. **102**, 722 (1956).
[10] J. H. Crawford, Jr., and J. W. Cleland, J. Appl. Phys. **30**, 1204 (1959).

Again reference points of 77 and 273°K were used for each sample.

CARRIER-REMOVAL RATE

The carrier-removal rate is found to be a function of the antimony concentration. Antimony-doped samples with concentrations of the order of 10^{13}, 10^{14}, and 10^{15} cm^{-3} showed carrier removal rates which increased with impurity concentration. These rates are listed in Table I. The values listed are the slopes of the curves

TABLE I. Carrier removal rate as a function of antimony concentration.

N_{Sb}^0	$\Delta_n/\Delta\phi$ at 77°K
1.074×10^{15}	7.09×10^{-4}
1.346×10^{14}	3.7×10^{-4}
1.051×10^{13}	1.032×10^{-4}

of carrier concentration versus exposure which were linear over the entire range of exposure at 77°K.

ISOCHRONAL ANNEALS

The isochronal annealing behavior for samples with antimony concentration of 1.074×10^{15} and 1.446×10^{14} cm^{-3} is shown in Fig. 1. There is little change in the carrier concentration of either sample in the temperature range below 273°K. Two annealing stages are observed above 273°K, one at about 300°K (stage A), and the second at about 400°K (stage B). The high-temperature process clearly dominates in the high-purity sample and the low-temperature process dominates in the low-purity sample. The annealing curves for the concentration of charged carrier scatterers, as represented by the reciprocal mobility, are very similar.

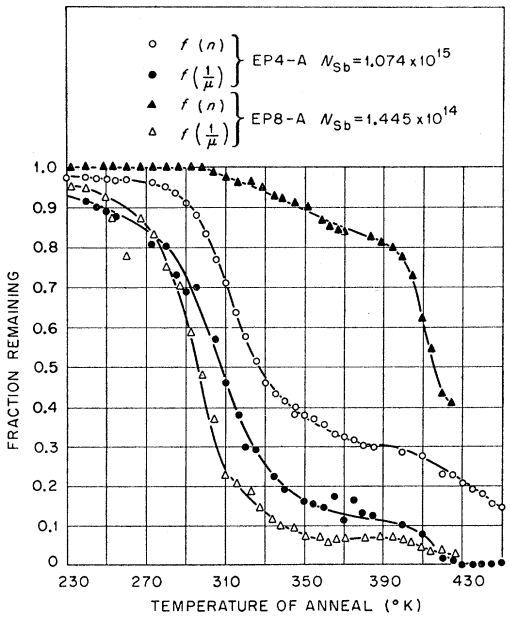

FIG. 1. Isochronal anneal after Co^{60} irradiation. Readings at 77°K after anneal.

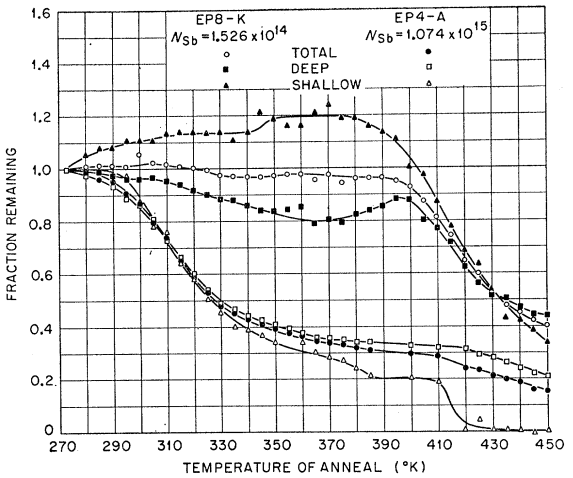

FIG. 2. Isochronal anneal after Co^{60} irradiation. Readings normalized to 273°K anneal.

Advantage is taken of the absence of major recovery below room temperature to determine the defect energy level distribution. From Hall coefficient measurements, it was found that the defect states were essentially the same as reported for room-temperature irradiations; namely, a set of shallow states at $E_c-0.2$ eV and a set of deep ones at or below the center of the band gap. The concentration of these two types of states was found to be essentially equal.

About 90% of the radiation induced change in the concentration of charged-scattering centers, as represented by the fractional change in reciprocal mobility $f(1/\mu)$, recovers in stage A for both the high-purity and low-purity samples. There is only about a 20% recovery of the fractional change in carrier concentration, $f(n)$ for the high-purity sample in stage A in contrast to 70 to 80% recovery for the low-purity samples in this stage. This suggests that some process in which positive- and negative-charged centers are paired occurs in stage A as a parallel and distinctly different process to defect removal. The annealing in Stage B for the high-purity sample is then primarily defect removal since the process causing the change in $f(1/\mu)$ has essentially gone to completion in stage A. It can be seen from Fig. 1 that stage B can be studied for the high-purity sample by anneals in the temperature range from 350 to 450°K.

An isochronal anneal of a second sample cut from the high-purity ingot and irradiated as before is shown in Fig. 2. Since there is a negligible amount of annealing below 273°K, as seen in the previous sample (Fig. 1), the Hall coefficient and resistivity characteristics were measured for the temperature range from 77 to 273°K before starting the anneal. Consequently, it was possible to study the change in concentration of both

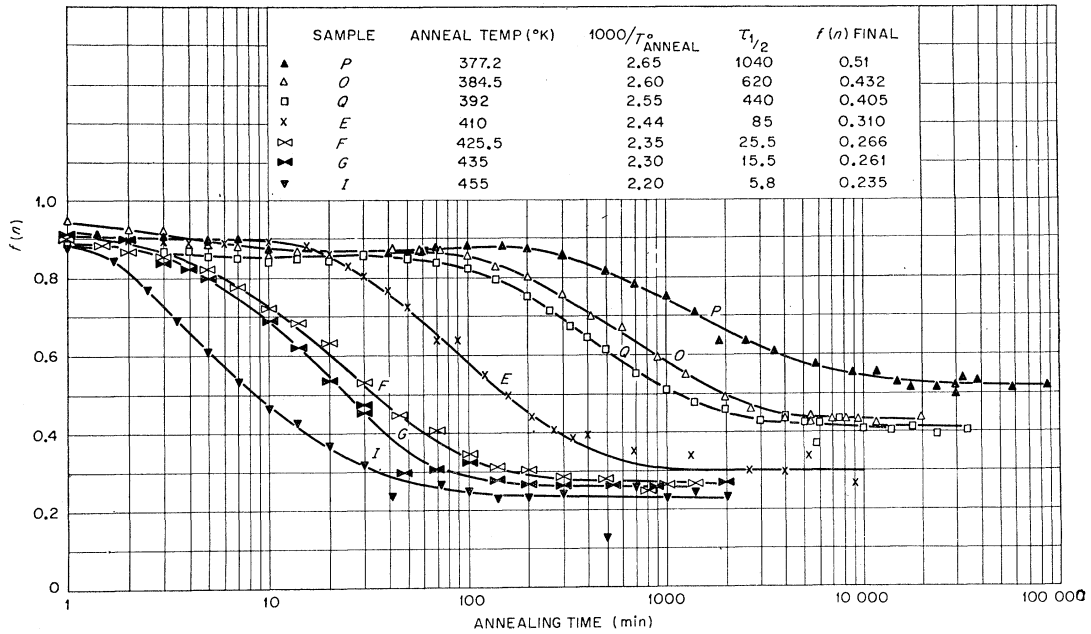

FIG. 3. Summary of isothermal annealing curves measured at 77°K.

the deep and shallow states as well as the total state concentration. To permit a direct comparison of the data of the former low-purity sample with a high-purity sample, the data from the low-purity sample has been normalized by setting $f(n)$, taken after the 273°K anneal, equal to unity.

The deep and shallow states anneal together in the low-purity sample up to about 410°K. The shallow states are removed rapidly above 410°K. There is no such correlation in stage A for the anneal of the high-purity sample. The deep states anneal slowly, then recover, showing a minimum at about 365°K. The shallow state concentration exhibits a gradual increase in the domain of stage A up to ~380°K.

The increase in shallow-state concentration at 350°K apparently results from the introduction of a new shallow state at 0.09 eV below the conduction band. This 0.09-eV level, which will be discussed in more detail later, appears at about 350°K and does not anneal for the temperature range employed in these experiments. The shallow states and the deep states recover together for the high purity sample in stage B. It is clear from the data of Figs. 1 and 2 that the antimony concentration strongly influences the annealing process.

ISOTHERMAL ANNEALS

Samples cut from the ingot with an antimony concentration of $\sim 1.4\times10^{14}$ cm^{-3} were irradiated at liquid-nitrogen temperature until ~90% of the conduction-electron concentration had been removed. They were then annealed isothermally in the temperature range between 377 and 455°K. The data are summarized in Fig. 3.

In every case there was a rapid annealing which removed ~10% of the induced-carrier change. There was then a second anneal which constituted the major recovery, after which the process saturated and the carrier concentration remained constant against further annealing. The major anneal occurred at longer times for lower temperatures, as is to be expected. It can also be seen that the saturation plateau was higher for lower temperatures.

After the completion of the anneal of sample P at 377°K, the temperature of the oil bath was increased to 455°K, and a second anneal was attempted at this higher temperature. It was expected that the plateau would move from the value attained at 377°K to a value characteristic of a 455°K anneal, such as was observed for sample I. There was no change, however, in the plateau value of $f(n)$ after a cumulative heating for 6 h at 455°K. Sample 0 was also annealed at 455°K for several hours after reaching its plateau at 384°K and a similar result was obtained. One may conclude, therefore, that the arrangement of defects produced by annealing is a function of the conditions of the anneal and, once produced, it is stable against further heating in the temperature range studied. A plot of $\tau_{1/2}$, the time required for the major annealing process to go halfway to completion, as a function of the reciprocal of the annealing temperature, is shown in Fig. 4 for stage B. The curve has two branches with apparent activation energies of 1.2 and 0.8 eV for the lower and higher temperature segments, respectively.

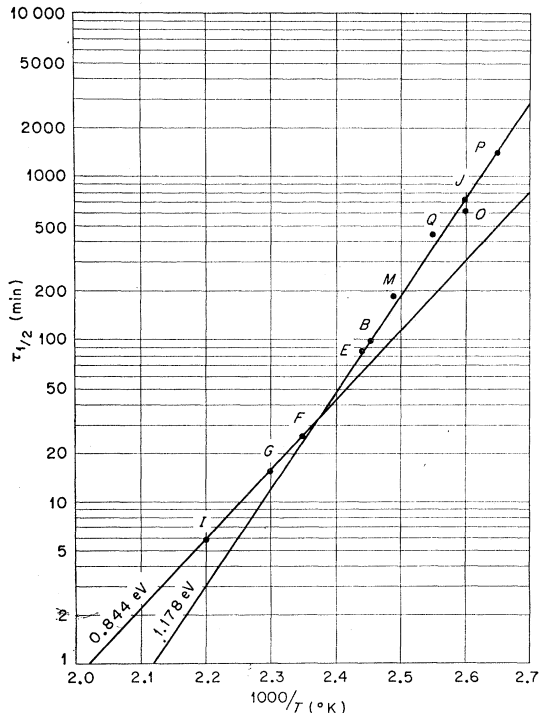

FIG. 4. Time to 50% anneal of total state concentration.

A typical isothermal anneal showing the behavior of the deep and shallow states for a high-temperature anneal is shown in Fig. 5. The shallow and deep states anneal together. After 2000 min of annealing at 455°K, ~20% of the shallow-state concentration is still present. This is in contrast to the behavior of lower purity samples, in which all of the shallow-state concentration was removed after 20 min at 410°K. A typical isothermal anneal for the low-temperature range is shown in Fig. 6. The shallow level again saturates with about 20% remaining. An increase in the deep-state concentration is observed during the early stages of the anneal. This is in agreement with the observations from the samples which were isochronally annealed (Fig. 2). The deep state saturates with about 70% of the induced change remaining.

The temperature dependence of the Hall constant before irradiation, after irradiation, and at various times during an isothermal anneal is shown in Fig. 7. This refers to the same sample whose anneal is shown in Fig. 6. The times at which the Hall measurements were made are indicated in the figures. The curve taken after irradiation shows no structure for values of $1000/T$ between 6 and 13. After a 70-min anneal at 377.2°K, a level has appeared at $E_c-0.09$ eV. The change in carrier concentration associated with this level (8×10^{12} cm^{-3}) remains essentially constant throughout the remainder of the anneal. This effect was observed in all of the samples studied. Another sample cut from the same ingot was heated in air at 600°C for 18 h. It was then irradiated at liquid-nitrogen temperature until the Hall constant was the same as that of the sample shown in Fig. 7. After which the sample was then annealed for 70 min at 377.2°K. The change in carrier concentration associated with the 0.09-eV level in this sample was approximately twice that observed before high-temperature-oxygen heat treatment.

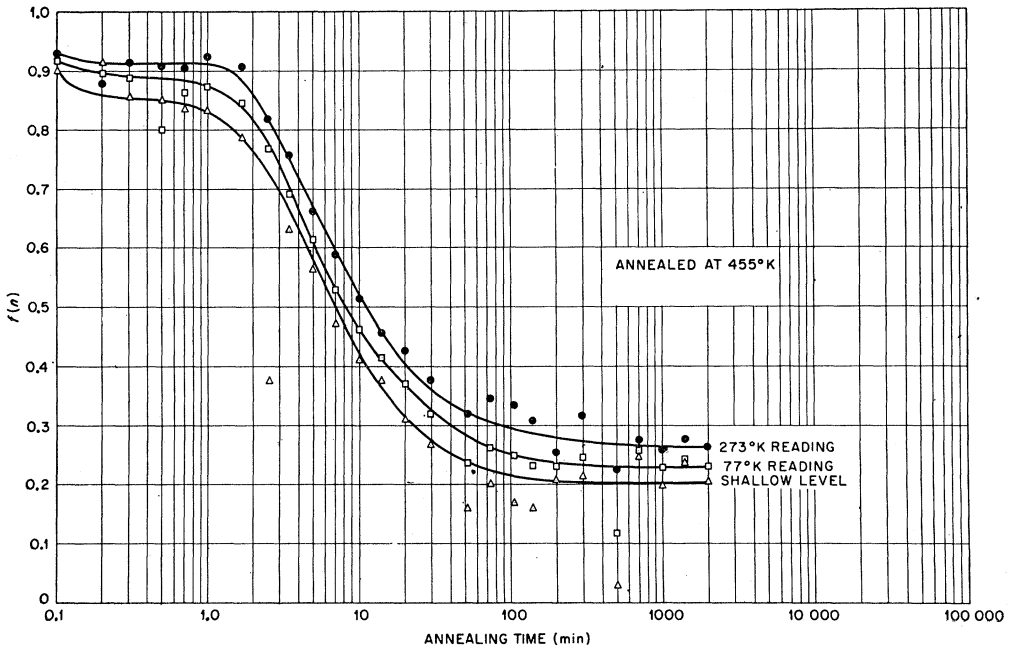

FIG. 5. An isothermal anneal in the high-temperature range.

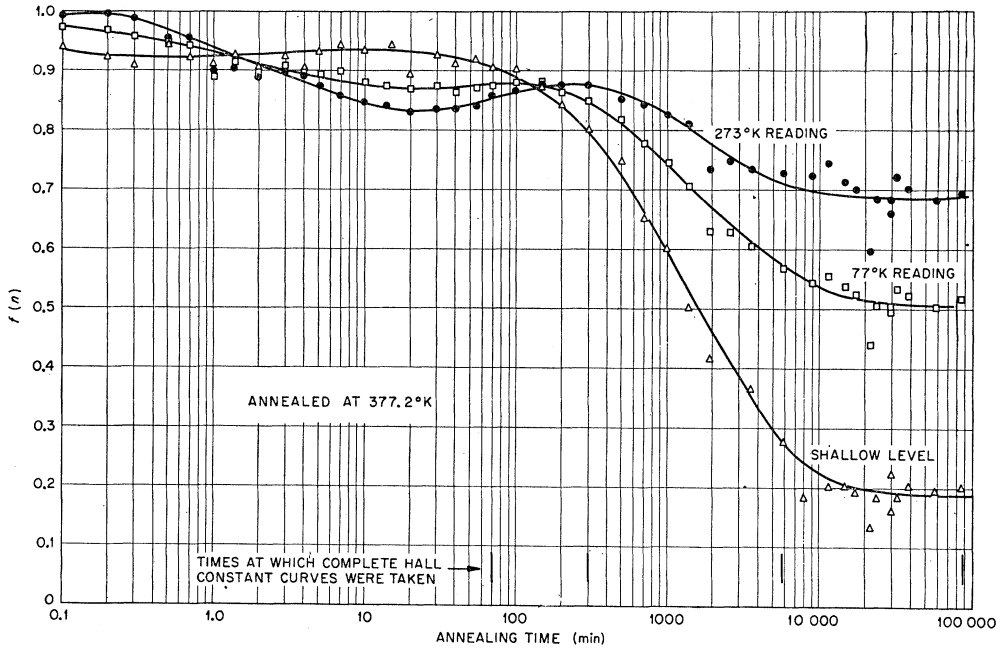

FIG. 6. An isothermal anneal in the low-temperature range.

Since an anneal at this temperature in oxygen would be expected to increase the concentration of dissolved oxygen in the specimen, we tentatively conclude that the 0.09-eV state is associated with a vacancy-oxygen complex (an oxygen atom occupying a vacancy). The state would then be analogous to the thermally stable oxygen-vacancy state at 0.17 eV observed in electron-bombarded silicon. Recently, vacancy-oxygen complexes in electron irradiated germanium deliberately doped with oxygen have been detected by means of infrared absorption.[11] It would be interesting to determine whether these defects revealed by their optical absorption band also possess a level at 0.09 eV.

DISCUSSION

The two principal energy-level models proposed for the irradiation introduced defects in germanium are those of James and Lark-Horovitz[12] and Blount.[13] These models which treat the charge states of the Frenkel defect (interstitials and vacancies) were considered by Ishino *et al.*[8] in the treatment of their data. On the other hand Watkins, Corbett, and co-workers[1–3,5] have found that the irradiation-induced levels in silicon can be explained without recourse to the interstitial, i.e., in terms of the vacancy and the interactions of the vacancy with the other atoms present in the sample. In view of the similarity between the silicon and germanium lattice, it is tempting to try to explain the behavior of irradiation-induced defects in germanium in terms of vacancies and vacancy complexes also. In this paper we will discuss the annealing of the radiation defects in terms of the interactions of the various species present in the crystal. In our following discussion it will be assumed that the interstitials will have migrated to sinks at the temperature of the irradiation and the defects responsible for electronic changes observed subsequent to irradiation and also annealing involve vacancies either free or in complexes.

Comparison of $f(1/\mu)$ and $f(n)$ for the high-purity sample in Fig. 1 indicates that a large change in the concentration of charged scattering centers introduced by bombardment occurred without a corresponding change in carrier concentration. This fact would suggest that positive- and negative-charge centers become paired, which would take place if a negatively charged vacancy were to migrate into the vicinity of a positively charged antimony atom. Such a process would be consistent with the previous observations that the impurity atom influences the annealing behavior.[6,7] This pairing alone, however, is unable to explain the fact that the major anneal occurs in stage B nor can it explain the existence of the thermally stable saturation plateau.

The behavior of the saturation plateau suggests that some species is formed in the annealing process which has a deep state and, once formed, is stable in the temperature range studied. Moreover, it appears that one of the reactants leading to the formation of this

[11] R. W. Whant and H. J. Stein, Appl. Phys. Letters **3**, 187 (1963).
[12] H. James and K. Lark-Horovitz, Z. Physik. Chem. **198**, 107 (1951).
[13] E. I. Blount, Phys. Rev. **113**, 995 (1959); J. Appl. Phys. **30**, 1218 (1959).

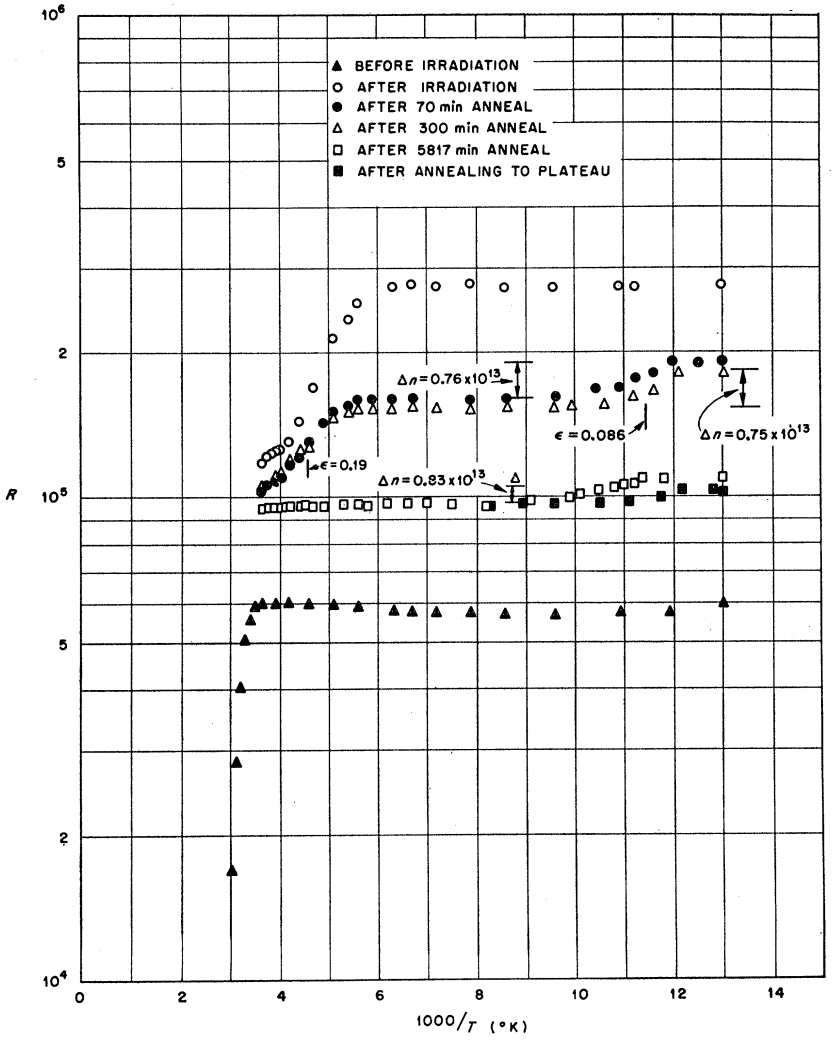

FIG. 7. Temperature dependence of the Hall constant during an isothermal anneal in the low-temperature range.

species decreases in concentration with increasing temperature, otherwise the saturation plateau would not decrease with increasing temperature.

A possible explanation for the plateau would be the formation of an antimony-divacancy complex. The Coulomb barrier between the negatively charged vacancies would be relaxed by the formation of the antimony-vacancy complex, thus permitting the vacancies to approach each other. The binding energy of the complex, by analogy with the findings of Watkins and Corbett[1,3] on silicon, would be expected to be rather high.

The sinks for eventual annihilation of the defects are probably associated with the dislocations present in the sample. According to the model of Koehler, Seitz, and Bauerle,[14] the vacancies diffuse to the dislocations, become trapped in the strain field, and then diffuse rapidly along the dislocations to jogs at which they may be annihilated. Hence, the entire dislocation line may be considered to be an unsaturable sink. The dislocation line density in the material used was measured to be about 10^4 cm^{-3}.

The sequence of events governing the thermal annealing of vacancies then might be as follows:

(1) A vacancy (V) may diffuse to a lattice site adjacent to an antimony atom (Sb) forming a weakly bound antimony-vacancy complex (SbV). The reaction may be written:

$$V+Sb \underset{k_2}{\overset{k_1}{\rightleftharpoons}} SbV,$$

where k_1 denotes the rate constant for complex formation and k_2 that for the breakup.

(2) The antimony-vacancy complex may capture a second vacancy to form a highly stable antimony-

[14] J. S. Koehler, F. Seitz, and J. E. Bauerle, Phys. Rev. **107**, 1499 (1957).

divacancy complex (SbV_2):

$$V+SbV \xrightarrow{k_3} SbV_2,$$

where k_3 is the appropriate rate constant.

(3) A vacancy may be captured by a dislocation (D) and annihilated at a jog.

$$V+D \xrightarrow{k_4} 0.$$

Although the exponential coefficients are different, k_1, k_3, and k_4 are all proportional to $e^{-E_m/kT}$, where E_m is the energy of vacancy motion. k_2 is proportional to $\exp-(E_m+E_B)/kT$, where E_B is the binding energy of the SbV complex.

Denoting the concentration of each species by N with a subscript, the following differential equations may be written:

$$dN_V/dt=-k_1N_VN_{Sb}+k_2N_{SbV}-k_3N_VN_{SbV}-k_4N_VN_D, \quad (1)$$

$$dN_{Sb}/dt=-k_1N_VN_{Sb}+k_2N_{SbV}, \quad (2)$$

$$dN_{SbV}/dt=k_1N_VN_{Sb}-k_2N_{SbV}-k_3N_VN_{SbV}, \quad (3)$$

$$dN_{SbV_2}/dt=k_3N_VN_{SbV}. \quad (4)$$

The equation of conservation for the impurity atoms is given by:

$$N_{Sb}+N_{SbV}+N_{SbV_2}=N_{Sb}{}^0. \quad (5)$$

An approximate solution of this set of coupled equations can be accomplished by assuming process (1) to be essentially at equilibrium. One can write:

$$N_{SbV}=KN_{Sb}N_V, \quad (6)$$

where K is the equilibrium constant. The value of K will be a function of the binding energy of the antimony-vacancy complex.

Since the antimony-vacancy complex disappears either by breaking up into its components or by capturing a second vacancy to become an antimony-divacancy, its annealing kinetics must also be considered. Aside from the introduction of the 0.09-eV level due to oxygen, although the mobility changes are largely recovered during the early anneal (stage A), one cannot detect a change in energy structure. It is assumed therefore that the energy level structure of the antimony-vacancy complex is not greatly different from that of the isolated vacancy. One can define a total annealable concentration N_T as

$$N_T=N_V+N_{SbV}, \quad (7)$$

in which one can express N_V and N_{SbV} in terms of N_{Sb} and N_T from Eq. (6). Since $N_{Sb}\gg N_{SbV}$, N_{Sb} can be approximated by the initial antimony concentration $N_{Sb}{}^0$. Hence,

$$N_{SbV}=KN_{Sb}{}^0N_T/(1+KN_{Sb}{}^0), \quad N_V=N_T/(1+KN_{Sb}{}^0). \quad (8)$$

From Eqs. (1) and (3), one has

$$\frac{dN_T}{dt}=-\frac{2k_3KN_{Sb}{}^0N_T{}^2}{(1+KN_{Sb}{}^0)^2}-\frac{k_4N_DN_T}{1+KN_{Sb}{}^0}; \quad (9)$$

integration of which yields

$$N_T=\frac{bN_V{}^0e^{-bt}}{b+aN_V{}^0(1-e^{-bt})}, \quad (10)$$

where

$$a=2k_3KN_{Sb}{}^0/(1+KN_{Sb}{}^0)^2,$$
$$b=k_4N_D/(1+KN_{Sb}{}^0),$$

and $N_V{}^0$ is the initial vacancy concentration.

The time constant is given by b^{-1},

$$\tau=(1+KN_{Sb}{}^0)/k_4N_D. \quad (11)$$

At high temperatures where $KN_{Sb}{}^0\ll 1$, the value of τ is given by

$$\tau=1/k_4N_D. \quad (12)$$

Furthermore, providing $k_4N_D\gg 2k_3N_{Sb}{}^0K$, N_T can be approximated by

$$N_T=N_V{}^0e^{-k_4N_Dt}. \quad (13)$$

An expression of this form is to be expected for temperatures at which the antimony-vacancy complex is unstable since the annealing process would involve direct migration to sinks. The isothermal data show that the annealing behavior shifts to a first-order law of this type for the high-temperature anneals. On the other hand, at lower temperatures where $KN_{Sb}{}^0\gg 1$, τ is given by

$$\tau=KN_{Sb}{}^0/k_4N_D. \quad (14)$$

The shift in the value of τ with temperature is also shown in the isothermal data (Fig. 3). Expanding the exponential in terms of a small argument for low temperatures, the annealing shifts to a second-order law:

$$N_T=KN_{Sb}{}^0N_V{}^0/(KN_{Sb}{}^0+2k_3N_Vt^0). \quad (15)$$

The quantity observed is the fraction $f(n)$ of the induced change in carrier concentration remaining at any time. Since the antimony-divacancy ionization levels can also contribute to the change in carrier concentration, the value of $f(n)$ is given by

$$f(n)=(\alpha N_T+\gamma N_{SbV_2})/\alpha N_V{}^0, \quad (16)$$

where the coefficients of the concentrations are the respective ionization states. Analyses of the saturation plateaux for the readings at 77 and 273°K show that the ratio of ionization at these temperatures is also 2:1. Hence,

$$\alpha=2,\ \gamma=2 \text{ for } 77°K, \text{ and } \alpha=1,\ \gamma=2 \text{ for } 273°K.$$

It is necessary, therefore, also to determine N_{SbV_2}.

Substitution of Eq. (8) into Eq. (4) yields

$$dN_{SbV_2}/dt=k_3KN_{Sb}{}^0N_T{}^2/(1+KN_{Sb}{}^0)^2, \quad (17)$$

which yields upon integration

$$N_{SbV_2}=\frac{N_V{}^0}{2}\left\{\frac{(b+aN_V{}^0)(1-e^{-t/\tau})}{b+aN^0{}_V(1-e^{-t/\tau})}\right\} -\frac{b}{2a}\ln\left[1+\frac{aN_V{}^0}{b}(1-e^{-t/\tau})\right].$$

The maximum value that N_{SbV_2} can attain for any anealing temperature is $\frac{1}{2}N_V{}^0$, as would be expected from the fact that two vacancies are required to form the stable complex.

The value of $f(n)$ then becomes

$$f(n)=\frac{e^{-t/\tau}}{1+(aN_V{}^0/b)(1-e^{-t/\tau})}+\frac{1}{2}\frac{\gamma}{\alpha} \left\{\frac{(1+(aN_V{}^0/b))(1-e^{-t/\tau})}{1+(aN_V{}^0/b)(1-e^{-t/\tau})} -\frac{b}{aN_V{}^0}\ln\left[1+\frac{aN_V{}^0}{b}(1-e^{-t/\tau})\right]\right\}. \quad (18)$$

Obviously Eq. (18) provides for neither the loss of vacancies during stage A recovery (e.g., to oxygen-vacancy complexes) nor the residual-carrier concentration change after prolonged high-temperature anneal, which is presumably associated with these complexes and divacancies created directly during irradiation. Nevertheless, it accounts well for the major recovery and for the saturation plateau.

The temperature dependence of Eq. (13) enters through the relaxation time τ as defined in Eq. (11). It was pointed out that τ has two limiting ranges of behavior. The limiting approximations [Eqs. (12) and (14)] indicate that the apparent activation energy should approach E_m+E_B at low temperature and E_m at high temperature where E_m is the energy of motion of a free vacancy and E_B is the binding energy of the SbV complex. This is consistent with the observed behavior of Fig. 4 which indicates a higher activation energy at low temperature than high temperature. From these data one can conclude that $E_m<0.84$ eV and $E_B>0.34$ eV. More extensive information on stage B annealing which covers a wider temperature range is required to fix values of E_m and E_B more exactly by such an approach. However, E_m should also be the activation energy for stage A and other work indicates[6-8] this to be 0.75 to 0.80 eV. In addition, one can show from Eq. (6) that values of N_{SbV} required to make this annealing model valid correspond to a value of $E_B>0.5$ eV. Hence, $E_m+E_B\simeq 1.3$ eV, which is in good agreement with the activation energy reported by Ishino *et al.* for an analogous annealing situation.

Thus far only the low donor concentration ($N_{Sb}{}^0 \sim 10^{14}$ cm^{-3}) recovery behavior has been considered. As shown in Figs. 1 and 2, the isochronal recovery of specimens containing $\sim 10^{15}$ antimony atoms cm^{-3} is markedly different. Therefore, before credence can be given the model proposed above, one must ascertain whether it contains provision for this difference in behavior or whether the difference arises from other factors which do not conflict with the model as stated. It was noted earlier that the more impure specimen ($N_{Sb}{}^0 \simeq 10^{15}$ cm^{-3}) corresponds closely in behavior with the results obtained by Brown *et al.* for specimens with similar carrier concentrations, i.e., the recovery of carrier concentration is dominated by stage A, in which $\sim 70\%$ of the electrons are restored before stage B begins. On the other hand, the behavior of the high-purity specimens is consistent with the observations of Ishino *et al.* who find that for $N_{Sb} \sim 10^{14}$ cm^{-3}, the annealing of defect acceptors is dominated by stage B. They are also consistent with the recovery of lifetime in irradiated high purity *n*-type germanium.

It has been found that the small stage A anneal (~ 10 to 20% recovery in carrier concentration) in high purity specimens is accompanied by the formation of an approximately equivalent number of 0.09-eV states, and is accompanied by $\sim 50\%$ recovery of mobility. Therefore, the loss of vacancies by migration to sinks during this stage seems to be small even though the vacancies are able to move to impurity atoms to form oxygen-vacancy and antimony-vacancy complexes. In the more impure specimens (as can be seen in Fig. 1), although the relative recovery in $1/\mu$ is somewhat greater than that of n, destruction of defects responsible for both acceptor states and carrier scattering seems to dominate stage A. The Hall coefficient versus temperature curves for this specimen reveal that loss of acceptor states through oxygen-vacancy complex formation cannot account for the annealing. This is also seen in Fig. 2, in which it is apparent that the deep and shallow states recover together.

The question then is how can an increase in N_{Sb} enhance the ease with which radiation defects (presumably vacancies) can be annihilated. In terms of the model proposed above, one would expect the increase of donor density to increase the thermal stability of the antimony-vacancy complexes through the law of mass action and, thereby, to increase the probability of antimony-divacancy formation in stage B relative to the higher purity specimens. Thus, one is forced to conclude that either the model is incorrect or that some entirely different process is favored by the higher antimony concentration.

Consideration of all factors suggests that the second alternative is the correct one. In addition, the extraneous process requires that the antimony impurity participate in some manner in the vacancy annihilation process. The simplest way for this to occur is for

the antimony atoms to act as vacancy sinks or annihilation sites, which implies that they must occupy interstitial positions. Obviously, the probability of preferential displacement of antimony atoms by the γ-irradiation is much too small to produce an appreciable concentration of antimony interstitials. Hence, if they are indeed present, some other means of creation must be responsible. The most likely means would seem to be by the interaction of a germanium interstitial with a substitutional antimony atom. An exchange process of this type would be highly probable if germanium interstitials migrate by interstitialcy motion, i.e., by successive replacement of adjacent atoms on lattice sites, and provided the interstitial atoms migrate at low temperature (activation energy for motion is small).

This hypothesis implies the following: Subsequent to the creation of an interstitial-vacancy pair by the incident radiation, the interstitials may (a) annihilate vacancies, (b) displace impurity (antimony) atoms into interstitial sites, or (c) move to other sinks such as dislocation jogs or interstitial platelets. Hence, the concentration of interstitial antimony atoms available to act as vacancy annihilation sites at higher temperatures would increase with increasing $N_{Sb}{}^{0}$. In addition, the proposed interaction of germanium interstitials with impurity atoms would in effect increase the total interstitial-sink concentration and, to the extent that the yield of defects depends upon competition between vacancies and interstitial sinks for migrating interstitials, would increase the apparent rate of defect introduction by the radiation, which is consistent with the observed (Table I) results.

The hypothesis that the different annealing behavior of heavily doped specimens from that of lightly doped ones is due to preferential annihilation of vacancies at interstitial antimony atoms is, of course, speculative. Experiments designed to test the model further are now underway.

In summary, the results reported here and previously by others suggest the following sequence of events during and subsequent to irradiation of antimony-doped specimens at 77°K. (1) Interstitial vacancy pairs are created by the irradiation, (2) relaxation of the interstitials occurs during irradiation, i.e., interstitials move to sinks and annihilate a portion of the vacancies. If the antimony concentration is high, an appreciable fraction of interstitials interact to produce interstitial antimony at the irradiation temperatures. It may be possible to account for the difference in response between antimony- and arsenic-doped specimens reported by Brown *et al.* at this step in terms of the difference in radius r of the substitutional atom ($r_{Sb} > r_{Ge} > r_{As}$). Since little lattice strain is associated with substitutional arsenic, the range of interaction with a moving interstitial would be much smaller than with the much larger antimony atom. (3) Upon warming to room temperature, the vacancy begins to move. During this period, which comprises stage A, vacancies migrate to annihilation sites on dislocations and at interstitial antimony atoms and they interact with substitutional antimony atoms and oxygen impurity to form antimony-vacancy and oxygen-vacancy complexes, respectively. (4) Upon heating to temperatures near 370°K, the vacancies stored in the form of antimony-vacancy complexes are released as these entities thermally dissociate (stage B). The free vacancies may migrate to dislocation sinks or interact with antimony-vacancy complexes to form highly stable antimony-divacancy complexes. The remaining stable complexes presumably anneal at higher temperatures (stage V of Ishino *et al.*)